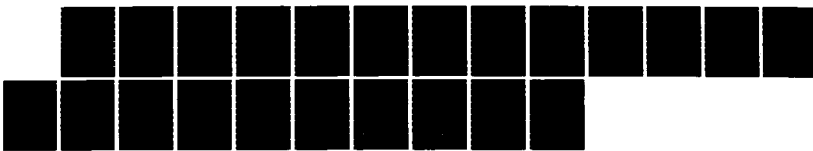
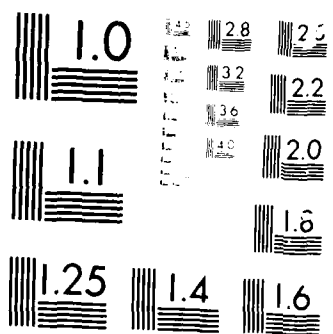


AD-A168 596 THE SYSTEMATICS OF THE STRUCTURES OF TERNARY COMPOUNDS 1/1
USING PSEUDOPOTENTIAL-ORBITAL RADII(U) CHICAGO UNIV IL
DEPT OF CHEMISTRY J K BURDETT 11 APR 86

UNCLASSIFIED N00014-85-K-8354

F/G 28/2 NL





100

AD-A168 596

SECURITY CLASSIFICATION OF THIS PAGE

REPORT DOCUMENTATION PAGE

1a. REPORT SECURITY CLASSIFICATION		1b. RESTRICTIVE MARKINGS										
2a. SECURITY CLASSIFICATION AUTHORITY		3. DISTRIBUTION AVAILABILITY OF REPORT Approved for Public Release: Distribution Unlimited										
2b. DECLASSIFICATION/DOWNGRADING SCHEDULE												
4. PERFORMING ORGANIZATION REPORT NUMBER(S)		5. MONITORING ORGANIZATION REPORT NUMBER(S)										
6a. NAME OF PERFORMING ORGANIZATION University of Chicago Jeremy K. Burdett	6b. OFFICE SYMBOL (If applicable)	7a. NAME OF MONITORING ORGANIZATION Dr. R.C. Pohanka										
6c. ADDRESS (City, State and ZIP Code) 5802 S. Ellis Avenue Chicago, Illinois 60637		7b. ADDRESS (City, State and ZIP Code) Office of Naval Research Code 3900 Arlington, Virginia 22217-5000										
8a. NAME OF FUNDING/SPONSORING ORGANIZATION	8b. OFFICE SYMBOL (If applicable)	9. PROCUREMENT INSTRUMENT IDENTIFICATION NUMBER N00014-85-K-0354										
9c. ADDRESS (City, State and ZIP Code)		10. SOURCE OF FUNDING NOS. <table border="1"><tr><td>PROGRAM ELEMENT NO.</td><td>PROJECT NO.</td><td>TASK NO.</td><td>WORK UNIT NO.</td></tr><tr><td>NR</td><td>700</td><td>003</td><td></td></tr></table>		PROGRAM ELEMENT NO.	PROJECT NO.	TASK NO.	WORK UNIT NO.	NR	700	003		
PROGRAM ELEMENT NO.	PROJECT NO.	TASK NO.	WORK UNIT NO.									
NR	700	003										
11. TITLE (Include Security Classification) The systematics of the structures of ternary NR systems using pseudopotential orbital radii		12. PERSONAL AUTHOR(S) J.K. Burdett										
13a. TYPE OF REPORT Annual	13b. TIME COVERED FROM 4-15-85 TO 4-1-86	14. DATE OF REPORT (Yr., Mo., Day) 4-1-86	15. PAGE COUNT									
16. SUPPLEMENTARY NOTATION												
17. COSATI CODES <table border="1"><tr><th>FIELD</th><th>GROUP</th><th>SUB GR.</th></tr><tr><td></td><td></td><td></td></tr><tr><td></td><td></td><td></td></tr></table>		FIELD	GROUP	SUB GR.							18. SUBJECT TERMS (Continue on reverse if necessary and identify by block number) structures, solids, stability	
FIELD	GROUP	SUB GR.										
19. ABSTRACT (Continue on reverse if necessary and identify by block numbers) Pseudopotential radii are used to sort ternary systems. By and large the sorting is only slightly better than that found using ionic radii, although the use of a third parameter allows sorting of the spinel and Cr ₃ S ₄ types.												
20. DISTRIBUTION/AVAILABILITY OF ABSTRACT UNCLASSIFIED/UNLIMITED <input type="checkbox"/> SAME AS RPT <input type="checkbox"/> DTIC USERS <input type="checkbox"/>		21. ABSTRACT SECURITY CLASSIFICATION										
22a. NAME OF RESPONSIBLE INDIVIDUAL		22b. TELEPHONE NUMBER (Include Area Code)	22c. OFFICE SYMBOL									

86 6 6 128

JUN 10 1986

The systematics of the structures of ternary compounds using pseudopotential-orbital radii

Accession For	<input checked="" type="checkbox"/>
NTIS GP&GI	<input type="checkbox"/>
DTIC TAB	<input type="checkbox"/>
Unclassified	<input type="checkbox"/>
Justification	
By Distribution	
Availability Codes	
- General or Specific	
First Special	

1. Introduction

Structural sorting diagrams have a long history of providing a qualitative understanding of the factors which determine the crystalline structure of a solid of given composition. The diagrams (usually, but not necessarily, two dimensional), are constructed by judiciously choosing two indices to represent the factors thought to determine the structure, and plotting the values of these parameters for every known solid in the isostoichiometric group. If the diagram can be neatly subdivided into regions corresponding to different structural types, then, for a sufficiently large database, it can be inferred that the indices do indeed represent, either directly or indirectly, the major factors which determine the structure. Well known examples of successful structural sorting diagrams are, for example, those constructed by Mooser and Pearson (1959), which use the Pauling electronegativity difference, and the average principle quantum number as indices, and those of Phillips and van Vechten.

The wide variety of structures found within the various families of ternary systems (e.g. AB_2O_4 , ABO_3), have been analysed by Muller and Roy (1974) in terms of structural sorting diagrams, using the Shannon-Prewitt (1969) ionic radii r_+^A , r_+^B , as indices. These diagrams are reasonably successful, and so demonstrate the importance of size in determining these structures. However, ionic radii are not entirely satisfactory as sorting parameters, since the radii are coordination number and valence state dependent, and so the predictive value of such diagrams is limited. Recently, very successful structural sorting maps have been produced for a variety of structural problems using pseudopotential orbital radii as indices. These orbital radii are fundamental atomic parameters with many interpretive and practical advantages, as discussed below. In this work we construct structural sorting diagrams for the major ternary families using these orbital radii, and compare and contrast the results with the Muller and Roy (1974) ionic radii sorting diagrams. The results are used

to shed new light on several problems of structural preference.

2. Pseudo potential orbital radii as atomic parameters

Many of the characteristic behaviour patterns of different elements are determined by the electronic configuration of the atom and the way in which the valence electrons are bound to the atomic core. This suggests that very fundamental atomic parameters can be extracted from the quantum mechanical description of the atoms. One type of such parameters, which has been derived from non-local pseudopotential theory, (St. John and Bloch 1974; Zunger 1980), are the orbital radii r_ℓ ($\ell=0, 1, 2$ corresponding to s, p, d electrons respectively), defined as the crossing point of the non-local pseudopotential $V_\ell^{\text{eff}}(r)$, and is characteristic of the potential experienced by the valence electrons due to the core electrons. A set of these parameters for all non-transition elements has been derived from spectral data by St. John and Bloch (1974), and a set for all elements up to lanthanum has been calculated, ab-initio, by Zunger (1980). (We will be using Zunger's radii throughout, since a large number of ternary compounds contain transition elements).

Naturally, these atomic parameters are intimately related to the traditional atomic scales of size and electronegativity. The combination $r_\sigma = r_s + r_p$ is a measure of an average 'core size' of an atom, and indeed, for each row of the Periodic Table, r_σ scales with Pauling's tetrahedral radius (Zunger 1980b). The energetics of an atom also depend on the core electrons, and the values of $(r_\ell)^{-1}$ scale with the averaged multiplet ionisation energy of the ℓ th orbital (Zunger 1980b). Hence the sum $\chi = 1/r_s + 1/r_p$ is a measure, to some degree, of the electronegativity of atom in the Mulliken sense.

The pseudopotential radii, being atomic parameters, are obviously independent of coordination number and counterion, in sharp contrast to the ionic radii of Shannon and Prewitt (1969) which are used in the

sorting diagrams of Muller and Roy (1974). The ionic radii represent an apparent physical size, whereas the pseudopotential radii would appear to quantify the elemental trends in size in the periodic table.

For the transition metals, the orbital radii are also independent of oxidation state. However, for the heavy elements which exhibit the 'inert pair effect' (e.g. Pb, Tl), i.e. have variable valence because the outermost s electrons sometimes behave as if they were core electrons, the pseudopotential radii do depend on which electrons are defined as being in the core. It appears to be practically, as well as logically, necessary therefore to use the appropriate radii for the oxidation state for the elements which exhibit the inert pair effect, and the values used are given in Table 1. The effect of the outermost s electrons being included in the core is to considerably increase r_s and slightly decrease r_p , so the atom has a far larger "core size". The ionic radii have the same qualitative dependence on oxidation state.

Combinations of the r^A and r^B , designed to represent size mismatch between atoms A and B, and the orbital non-locality, were used to construct structural sorting diagrams for the AB octet and non-octet compounds (St. John and Bloch 1974; Zunger 1980). However, recent work (Burdett et al. 1981) has shown that excellent structural sorting for both the AB octet and AB_2 double octet compounds can be obtained by simply plotting the 'core size' of A and B as indices (i.e. r_σ^A against r_σ^B). Similar results can also be obtained using the electronegativity functions χ^A and χ^B , which demonstrates that the two views, that either 'size' or energetics is fundamentally important in determining structure, are closely linked via the properties of the core electrons.

It should be noted that with the orbital radii indices, as with all Mendeleyevian sorting diagrams, the boundaries between different regions can only be constructed *a posteriori*, at present. The prediction of boundary positions would require a more detailed quantitative understanding of the relationship between the orbital radii and the

energetics of solid formation than is available at the moment; though there is some evidence that the orbital radii can be used semi-quantitatively to analyse the energetics of solid state reactions (Burdett and Price 1981, Price et al. 1982). Also, it is significant that polymorphic compounds usually lie close to the boundaries on structural sorting diagrams (which attempt to use the zero temperature and pressure structure), indicating that the boundaries are physically reasonable, and indeed, often structures with surprisingly small energy differences can be resolved on such diagrams.

The pseudopotential indices r_{σ}^A and r_{σ}^B (or χ^A and χ^B) have also been used successfully to sort the inverse from normal spinels (AB_2X_4) with only four errors in a database of 172 known spinels (Price et al. 1982), which has interesting implications for the problem of cation distribution in spinels, particularly when contrasted with the crystal field stabilisation energy rationalisation which is often used.

The spinel cation distribution is a very special type of ternary structure problem, as the X-cation lattice is the same in both the normal and inverse structures, but the success of the sorting diagram approach in this case prompts the question as to whether the orbital radii are able to help in the understanding of the general structural problem in ternary compounds.

3. Results

The structural sorting diagrams were constructed using Zunger's radii (1980) and the database given in the appendix.

3.1 The AB_2O_4 structures.

For the 217 compounds plotted on the orbital radii sorting diagram (Figure 1), there is very good sorting, with all the spinel, $[K_2NiF_4]$ type, phenacite, olivine and $[CaFe_2O_4]$ type structures sorting well. The errors

in the sorting are

(i) The $[\text{Sr}_2\text{PbO}_4]$ structural region is poorly defined on the orbital radii map, particularly those examples which contain Cd, but is well defined on the ionic radii sorting map (Muller and Roy 1974).

(ii) All the $[\beta\text{-K}_2\text{SO}_4]$ plot in the same region, but Na_2CrO_4 , whose structure is closely related to $[\beta\text{-K}_2\text{SO}_4]$, is found in the spinel region. The compounds containing Tl with the $[\beta\text{-K}_2\text{SO}_4]$ structure plot in the correct region only if the inert pair effect is taken into account and the radii appropriate to Tl(I) used.

(iii) Cd_2SiO_4 is plotted on the boundary with the olivine region when it has the $[\text{Na}_2\text{SO}_4]$ structure.

(iv) The $[\text{Pb}_3\text{O}_4]$ structures are not plotted, and they would not be satisfactorily separated. This structure is very different from the others in this group, and can perhaps be best explained in terms of the structural and space filling effect of the lone pairs (P. B. Moore 1992) on the Group V elements.

This map is topologically similar to the ionic radii sorting map of Muller and Roy, and is equally successful. This emphasises the importance of "size" in determining these structures, and also the use of pseudopotential radii makes the diagram predictive.

4. The AB_2X_4 ($\text{X}=\text{S, Se, Te}$) family.

The orbital radii sorting diagram for the combined database for the other ternary chalcogenides is shown in Figure 2. Most of the structures sort well, but there is considerable overlap between the spinel and the $[\text{Cr}_3\text{S}_4]$ structures. This is a well known structural problem; the structures are related, being based on cubic and hexagonal anion packing respectively, and several systems transform for one structure to the other under suitable conditions. An approximate separation of the two structures

can be obtained using a third index R, defined

$R_3 = r_{\text{p}}^A + r_{\text{s}}^B - (r_{\text{p}}^X - r_{\text{s}}^S)$, demonstrating that the degree of covalency, ($r_{\text{p}} = r_{\text{p}} - r_{\text{s}}$ being an index of the hybridisation possibilities of the atomic orbitals), is important in determining which of the two structures will be adopted. A sorting of the two structures has also been obtained by Ohta and Anzai (1977) by using estimates of the dissociation energy and metal-metal bonding energies as indices. As Muller and Roy point out, all known $[\text{Cr}_3\text{S}_4]$ compounds contain transition metal ions with unfilled d electron shells, and short metal-metal distances have been observed in these compounds. Hence we can conclude that it is the covalent bonding possibilities which determine whether $[\text{Cr}_3\text{S}_4]$ or [spinel] is adopted, and this factor is not reflected in the $r_{\sigma}^A r_{\sigma}^B$ plots.

The other errors in Figure 2 are:

(i) Three spinels, CdY_2S_4 and $(\text{Mg}, \text{Cd})\text{Y}_2\text{Se}_4$ plot close to the $(\text{Mg}, \text{Mn})\text{Y}_2\text{S}_4$ structure, the $[\text{MnY}_2\text{S}_4]$ structure being more closely related to $[\text{CaFe}_2\text{O}_4]$. It is interesting to note that $(\text{Mg}, \text{Mn})\text{Tm}_2\text{S}_4$ are reported as having both the $[\text{MnY}_2\text{S}_4]$ and [spinel] structures.

(ii) Since the nature of the anion is not distinguished on this plot, the diagram does not resolve the different structures of CaY_2S_4 and CaY_2Se_4 , which adopt the $[\text{CaHf}_2\text{O}_4]$ structure.

(iii) The thiogallate structures are poorly resolved from the spinel structures. Muller and Roy excluded these compounds, along with $[\text{Pb}_3\text{O}_4]$, from their ionic radii sorting maps, on the grounds that these structures require covalent bonds so that the structures depend more on the electronic configuration of the atoms than their size. Presumably, the pseudopotential radii sorting maps fail to sort these structures for the same reasons, and since the two maps are so topologically similar, they are successful for the same reasons. The question arises as to how important is the nature of the anion in determining the structure. Comparing Figures 1 and 2 shows that the boundary lines for the olivine, spinel and $\beta\text{-K}_2\text{Si}_4$ are

are very similar for all the chalcogenides, though the larger anion lattices can accomodate larger cations in a given structure. This is supported by the large number of $AB_2(S,Se,Te)_4$ compounds containing lanthanides which are known, but unfortunately cannot be included in this study as the pseudopotential radii are not available. However, there are several structures which either occur only for the oxides, or only for the other chalcogenides, which is consistent with the more covalent structures being more sensitive to the nature of X.

5. Other results and conclusions

The ABO_3 compounds can be fairly well separated on a pseudopotential radii sorting diagram, but the ABO_4 family are not sorted satisfactorily. Since ABO_4 compounds must have at least A or B in oxidation state V or higher, or both be in oxidation state IV, these compounds involve a considerable amount of covalent bonding, and often include complex anions such as $(IO_4)^-$.

Hence it would appear that pseudopotential sorting diagrams for ternary compounds are successful when size is an important factor which will occur when the structure is fairly ionic with the cations fitting into different sites and slightly distorting the anion lattice. Thus these maps are very similar in form and interpretation to the ionic radii sorting diagrams.

For compounds where there is considerable covalent bonding, the electronic configuration of the atom will determine the possibilities for bonding to oxygen (and in some cases, the formation of metal-metal bonds), and so is the dominant factor in determining the structure. The AB octet and AB_2 double octet covalent compounds are sorted successfully, but this may be because the variation of r_p across a row of the periodic table can reflect the size and bonding properties adequately when A and B are in contact, and their oxidation states are related by an octet count. The

presence of a third element makes the 'bonding' possibilities more complicated, and also isolates A from B in the structure, and since r_σ, r_α -plots cannot reflect the important electronic factors, these pseudopotential plots (like the ionic radii plots), cannot sort the ternary structures which contain covalent bonds satisfactorily.

6. Acknowledgements.

We thank Dr.A. Bloch for supplying us with experimental values for the pseudopotential radii of elements which exhibit the lone pair effect.

7. References

Burdett JK, Price GD, Price SL (1981) The factors influencing solid state structures -an analysis using pseudopotential radii structural maps. Phys Rev B 24:2903-2912

Burdett JK, Price SL (1981) Heats of reaction in the solid state and their relationship to Bloch-Zunger structural diagrams. Phys Rev B 23:5642-5644

Mooser E, Pearson WB (1959) On the crystal chemistry of normal valence compounds. Acta Crystallogr 12:1015-1022

Moore PB

Muller O, Roy R (1974) The major ternary structural families. Springer, Berlin Heidelberg New York

Price GD, Price SL, Burdett JK (1982) The factors influencing cation site-

preferences in spinels. A new Mendelyvian approach. *Phys Chem Minerals* 8:69-76

Shannon RD, Prewitt CT (1969) Effective ionic radii in oxides and fluorides. *Acta Crystallogr B* 25:925-946

St John J, Bloch An (1974) Quantum-defect electronegativity scale for non-transition elements. *Phys. Rev. Lett* 33:1095-1098

Zunger A (1980a) Structural stability of 495 binary compounds. *Phys Rev Lett* 44:582-586

Zunger A (1980b) Systematization of the stable crystal structure of all AB type binary compounds: A pseudopotential orbital radii approach. *Phys Rev B* 22:5839-5872

8. Appendix: Database

The database was taken from Muller and Roy (1974) The low temperature and pressure structure is listed for compounds which are known to be polymorphic. Numbers in parentheses denote the number of structures in each group.

9. AB_2O_4 (217)

$[K_2SO_4]$ (33)

$(K,Rb,Cs,Tl)_2(S,Se)O_4$; K_2TeO_4 ; $(K,Rb,Cs,Tl,Ba)_2CrO_4$; $(K,Rb,Cs)_2(Mo,W)O_4$; $(Sr,Ba)_2(Si,Ge)O_4$; $Ba_2(Ti,Fe,Co)O_4$; $(K,Rb,Cs)_2MnO_4$; Tl_2WO_4 ; (Na_2CrO_4 is found in a closely related structure).

$[Na_2SO_4-V]$ (5)

$(Na,Ag)_2(S,Se)O_4$; Cd_2SiO_4

$[K_2NiF_4]$ (25)

$Ba_2(Pb,Zr,Hf,Sn,Ti)O_4$; $Sr_2(Zr,Hf,Sn,Mo,Tc,Ir,Ru,Ti,Rh,Fe,Mn)O_4$; Ca_2MnO_4 ; $(K,Rb,Cs)_2(U,Np)O_4$ (La radius used); $La_2(Ni,Cu)O_4$

$[Sr_2PbO_4]$ (7)

Sr_2PbO_4 ; $Ca_2(Sn,Pb,Ir)O_4$; $Cd_2(Pb,Sn,Pt)O_4$

Olivine (12)

$(Mg,Fe,Ca,Mn,Co,Ni)_2SiO_4$; $(Ca,Mn,Mg,Cd)_2GeO_4$; $BeAl_2O_4$; $BeCr_2O_4$

Phenacite (7)

$(Be,Zn)_2SiO_4$; $Li_2(W,Mo,Cr,Se)O_4$; Zn_2GeO_4

Spinels (95) (We do not distinguish between the normal and inverse structure here, the excellent sorting achieved has been discussed elsewhere (Price et al. 1982)).

$Na_2(Mo,W)O_4$; $Mg_2(Ge,Sn,Ti,V,Tc,Pd,Pt)O_4$; $Al_2(Mg,Cu,Zn,Mn,Fe,Co,Ni)O_4$; $Ga_2(Mg,Cu,Zn,Cd,Mn,Fe,Co,Ni)O_4$; $In_2(Mg,Cd)O_4$; Ag_2O_4 ; $Zn_2(Sn,Ti,V,Pt)O_4$

$Ti_2(Mg,Mn)O_4$; $V_2(Li,Mg,Zn,Cd,Mn,Fe,Co)O_4$; $Cr_2(Mg,Cu,Zn,Cd,Mn,Fe,Co,Ni)O_4$;
 $Mn_2(Li,Mg,Sn,Cu,Zn,Cd,Ti,V,Cr,Mn,Tc,Fe,Co,Ni)O_4$;
 $Fe_2(Mg,Ge,Cu,Zn,Cd,Ti,V,Cr,Mo,Mn,Fe,Co,Ni)O_4$;
 $Co_2(Ge,Sn,Zn,Ti,V,Mg,Cu,Mn,Tc,Fe,Co,Ni)O_4$; $Rh_2(Mg,Cu,Zn,Cd,Mn,Co,Ni)O_4$; Ni_2GeO_4

[CaFe₂O₄] (20) Many such compounds containing lanthanide elements have been omitted.

$(Ba,Sr)La_2O_4$; $Sr(Y,Sc,In)_2O_4$; $Ca(Sc,In,Rh,Fe,V,Cr)_2O_4$; $Ca(Ti,Mn)_2$; $SrTi_2O_4$;
 $BaIn_2O_4$; $La(Ti,V,Mn,Co,Ni)_2O_4$

[BaAl₂O₄] (7)

$(Sr,Ba,Pb)(Al,Ga)_2O_4$; $CaAl_2O_4$;

Borates (3)

$(Ca,Sr,Ba)B_2O_4$

[Pb₃O₄] Not plotted (9)

Pb_3O_4 ; Pb_2SnO_4 ; $Sb_2(Mg,Mn,Fe,Ni,Co,Zn)O_4$; As_2NiO_4

Unique Structures $[Sr_2CrO_4]$; $[Y_2BeO_4]$; $[Li_2SO_4]$

10. AB_2X_4 ($X=S, Se, Te$)

The many compounds of this type which contain lanthanide ions have been omitted.

[$\beta-K_2SO_4$] and closely related structures (15)

$(Cs,K,Rb)_2(W,Mo)S_4$; Cs_2WSe_4 ; Rb_2MoSe_4 ; $Ba_2(Sn,Si,Ge,Ti)S_4$; $Sr_2(Si,Se)S_4$; Pb_2GeS_4

Olivine (12)

$(Mg,Mn,Ca)_2(Si,Ge)S_4$; $(Mg,Ca)_2SnS_4$; Mg_2SnSe_4 ; $(Ca,Mg,Mn)_2SiSe_4$

Spinel (56)

$(Zn,Cr)Al_2S_2$; $CrGa_2S_4$; $(Co,Cu,Ni,Rh)Co_2S_4$; $(Co,Mg,Fe,Ni,Mn,Cd,Hg,Cr,Ca)In_2S_4$; $(Fe,Rh)Fe_2S_4$; $(Co,Fe,Ni,Rh)Ni_2S_4$; $ZnMn_2(S,Se)_4$; $(Zn,Co,Cu,Fe,Cd,Hg)Cr_2S_4$; $(Zn,Cu,Cd,Hg)Cr_2Se_4$; $CuCr_2Te_4$; CuV_2S_4 ; $(Co,Cu,Fe,Ni)Rh_2S_4$; $CuRh_2Se_4$; $CuTi_2S_4$; $(Co,Cu,Fe,Ni)Ir_2S_4$; $CuIr_2Se_4$; $(Zn,Mg,Fe,Mn)Sc_2S_4$; $(Mg,Mn)Sc_2Se_4$; $CuHf_2S_4$; CdY_2S_4 ; $(Mg,Cd)Y_2Se_4$

[$CaFe_2O_4$] (4)

$(Ba,Sr)Y_2(S,Se)_4$

[MnY_2S_4] (4)

CaY_2S_4 ; $(Mg,Mn,Cr)Y_2S_4$

[Th_3P_4] (9)

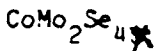
$La_2(Sr,Ba,Pb,La,Ca)S_4$; $La_2(Sr,Ba,Pb,La)Se_4$

[$CaHo_2Se_4$] (2)

$CaY_2(Se,Te)_4$

[Cr_3S_4] and related structures (60)

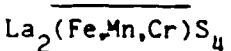
$(Co,Cu,Fe,V)Co_2Se_4$; $(Co,Fe,Ni,V,Cr,Ti)Fe_2Se_4$; $(Co,Fe,Ni)Ni_2Se_4$; $(Ni,Mn,V,Cr,Ti)Cr_2S_4$; $(Co,Fe,Ni,Cr,Ti)Cr_2Se_4$; $(Fe,V,Cr,Ti)Cr_2Te_4$; $(Co,Fe,Ni,V,Cr)V_2S_4$; $(Co,Fe,Ni,V,Cr)V_2Se_4$; $(V,Cr,Ti)V_2Te_4$; $(Co,Ni,Cr)Rh_2Se_4$; $(Cr,Rh)Rh_2Te_4$; $(Co,Fe,Ni,Cr,Ti)Ti_2S_4$; $(Co,Fe,Ni,V,Ti)Ti_2Se_4$; $(V,Cr,Ti)Ti_2Te_4$



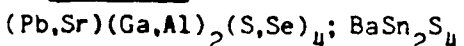
[Thiogallates] (17)

$\text{HgIn}_2(\text{Se},\text{Te})_4$; $\text{HgGa}_2(\text{S},\text{Se})_4$; $\text{HgAl}_2(\text{S},\text{Se},\text{Te})_4$; CdIn_2Te_4 ; $\text{CdGa}_2(\text{S},\text{Se},\text{Te})_4$;
 $\text{CdAl}_2(\text{S},\text{Se},\text{Te})_4$; $\text{ZnIn}_2(\text{Se},\text{Te})_4$; ZnAl_2Se_4

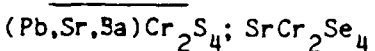
$[\text{La}_2\text{FeS}_4]$ (3)



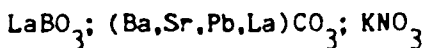
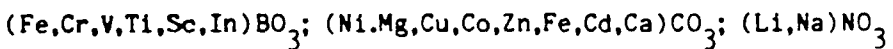
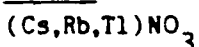
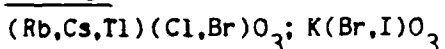
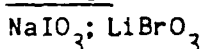
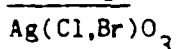
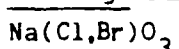
$[\text{PbGa}_2\text{S}_4]$ (9)



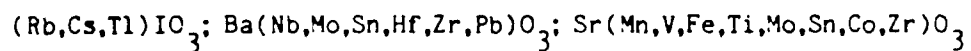
$[\text{PbCr}_2\text{S}_4]$ (4)



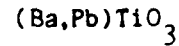
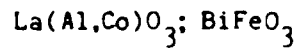
 11. ABO_3 systems VERY APPROXIMATE -CLOSE STUDY OF MULLER AND ROY REQUIRED

[Aragonite] (6)

[Calcite] (16)

[RbNO₃ -IV] (3)

[KBrO₃] (8)

[NaIO₃] (2)

[AgClO₃] (2)

[NaClO₃] (2)


Unique structures: $\text{LiIO}_3; \text{KCLO}_3; \text{YBO}_3$

[Cubic Perovskite] (17)


$(\text{Rb}, \text{K})\text{UO}_3$ and KTaO_3 also have this structure, but cannot be included on Figure 3W as no radii for the lanthanides are available.

[Tetragonal Perovskite] (2)

[Rhombohedral Perovskite] (3)

[GdFeO₃] (37)

$(La,Y)(Cr,Fe,V,Mn,Rh,Ti,Sc)O_3$; $La(In,Y)O_3$; $Ca(Mn,V,Ti,Ru,Tc,Mo,Nb,Sn,Hf,Zr)O_3$;
 $Sr(Ru,Ir,Hf,Zr,Pb,U,Ce)O_3$; $Na(Ta,Nb)O_3$; $Ag(Ta,Nb)O_3$

[Hexagonal Phases] (8)

$Ba(Ni,Co,Mn,Ru,Ir,Fe,V,Cr)O_3$

[PbZrO₃] (2)

$Pb(Zr,Hf)O_3$

[Pyroxenes]

$(Sr,Ba)GeO_3$

[Pyrochlores] (8)

$Pb(Ru,Ir,Tc,Sn)O_3$; $Bi(Sc,Y,Co,Ni)O_3$

[Al₂O₃] (3)

$(Al,Fe,Cr)_2O_3$

[Illmenite] (15)

$(Mg,Co,Mn,Fe,Ni,Zn,Cd)TiO_3$; $NiMnO_3$; $(Mg,Cd)SnO_3$; $CrAlO_3$; $NaSbO_3$; $(Cr,Fe)RhO_3$;
 $FeVO_3$

[Ordered Corundums] (3)

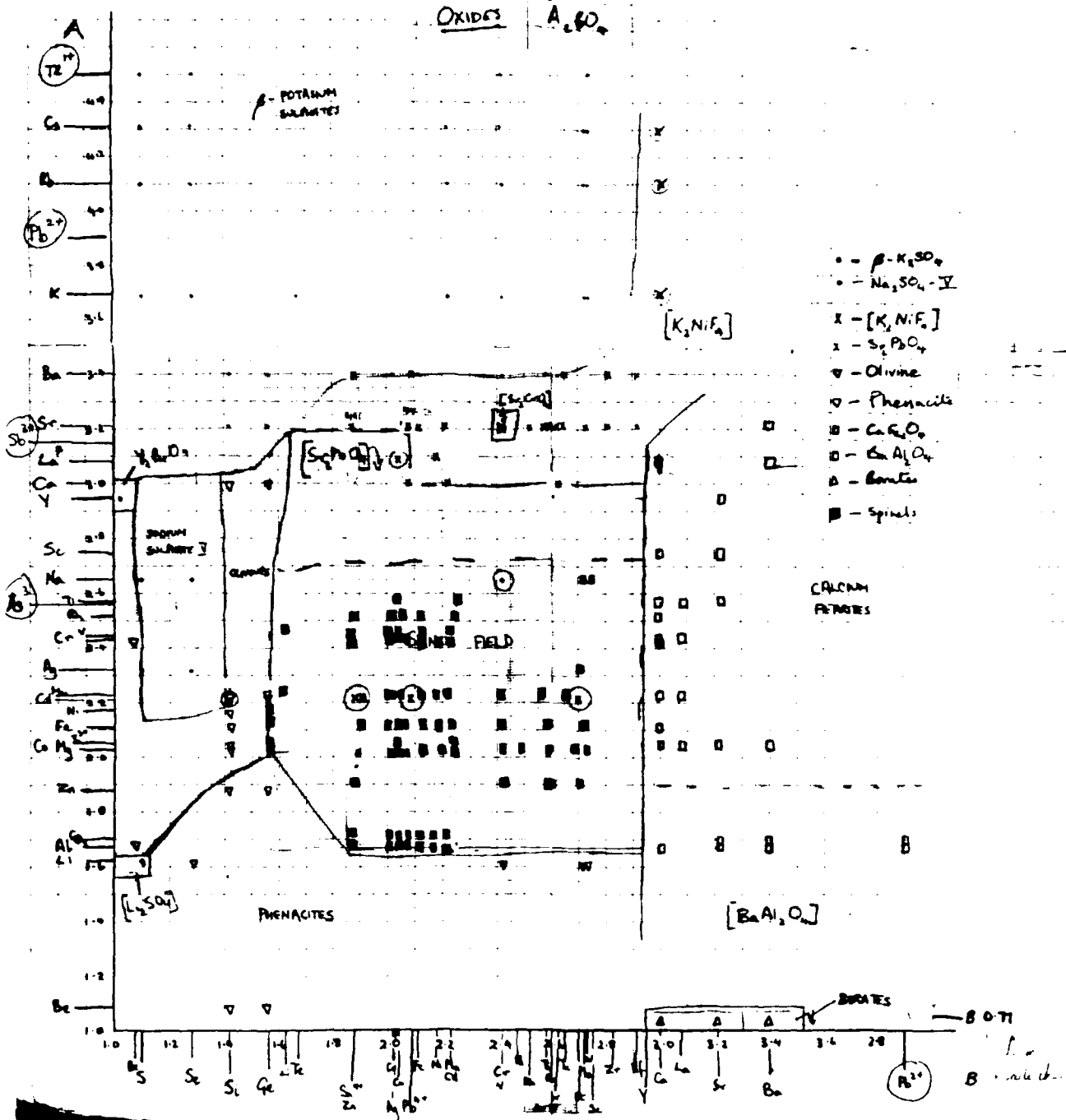
$Li(V,Ta,Nb)O_3$

Table 1. Pseudopotential radii for elements which exhibit variable valency because of the lone pair effect.

<u>Normal Valence Radii [Zunger 1980]</u>		<u>Inert pair valence radii</u>			
	r_s		r_s		
As(V)	0.67	0.745	As(III)	1.898	0.677
Sb(V)	0.83	0.935	Sb(III)	2.272	0.878
Bi(V)	0.92	1.077	Bi(III)	2.483	1.006
Pb(IV)	0.95	1.13	Pb(II)	2.837	1.065
Tl(III)	1.015	1.22	Tl(I)	3.442	1.137

The lower valence radii were obtained from Zunger's original radii by using the ratio of the experimental pseudopotential radii determined by Bloch (private communication).

e.g. $r_s(Pb^{II}) = r_s(Pb^{IV}) \times (r_s(Pb^{II})/r_s(Pb^{IV}))^{\text{exp}}$

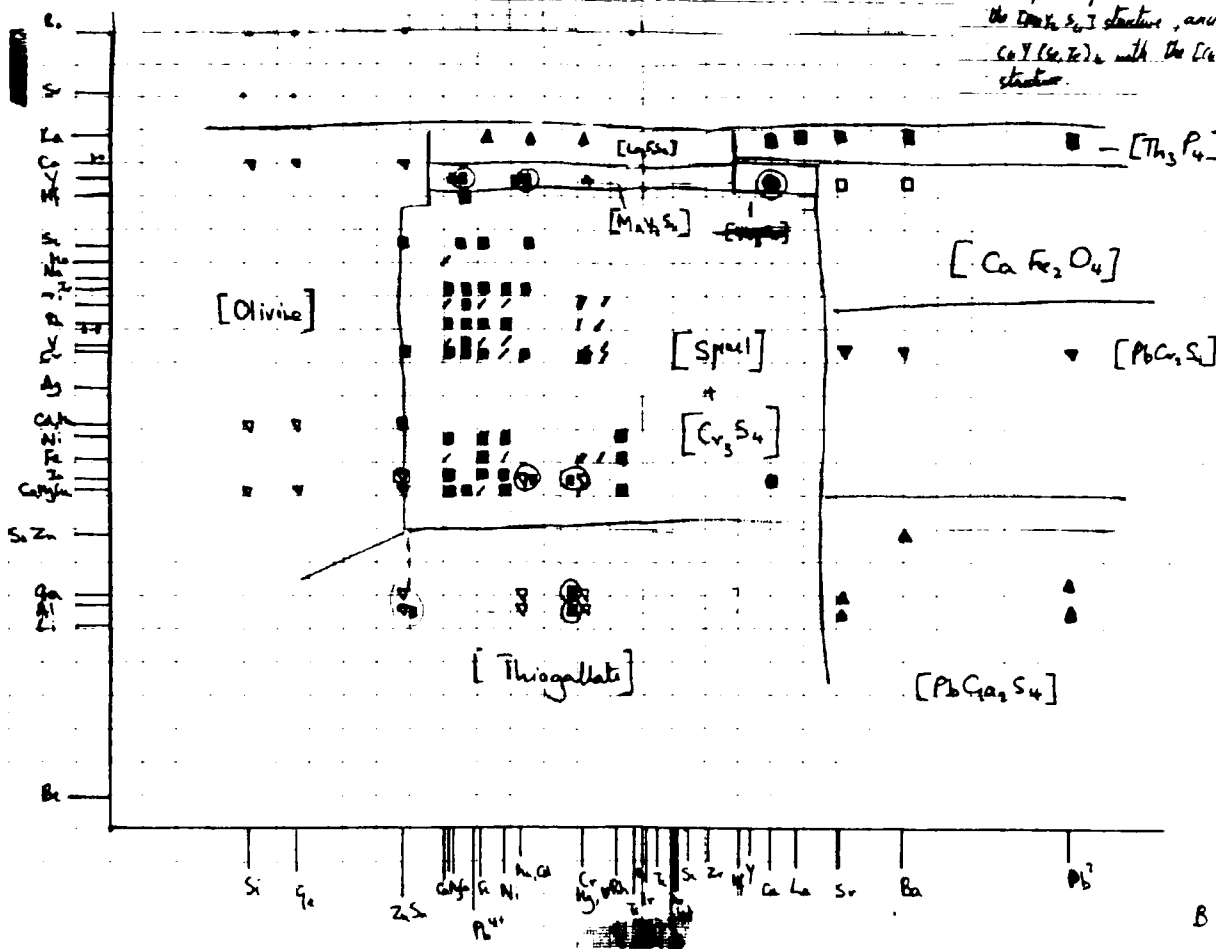


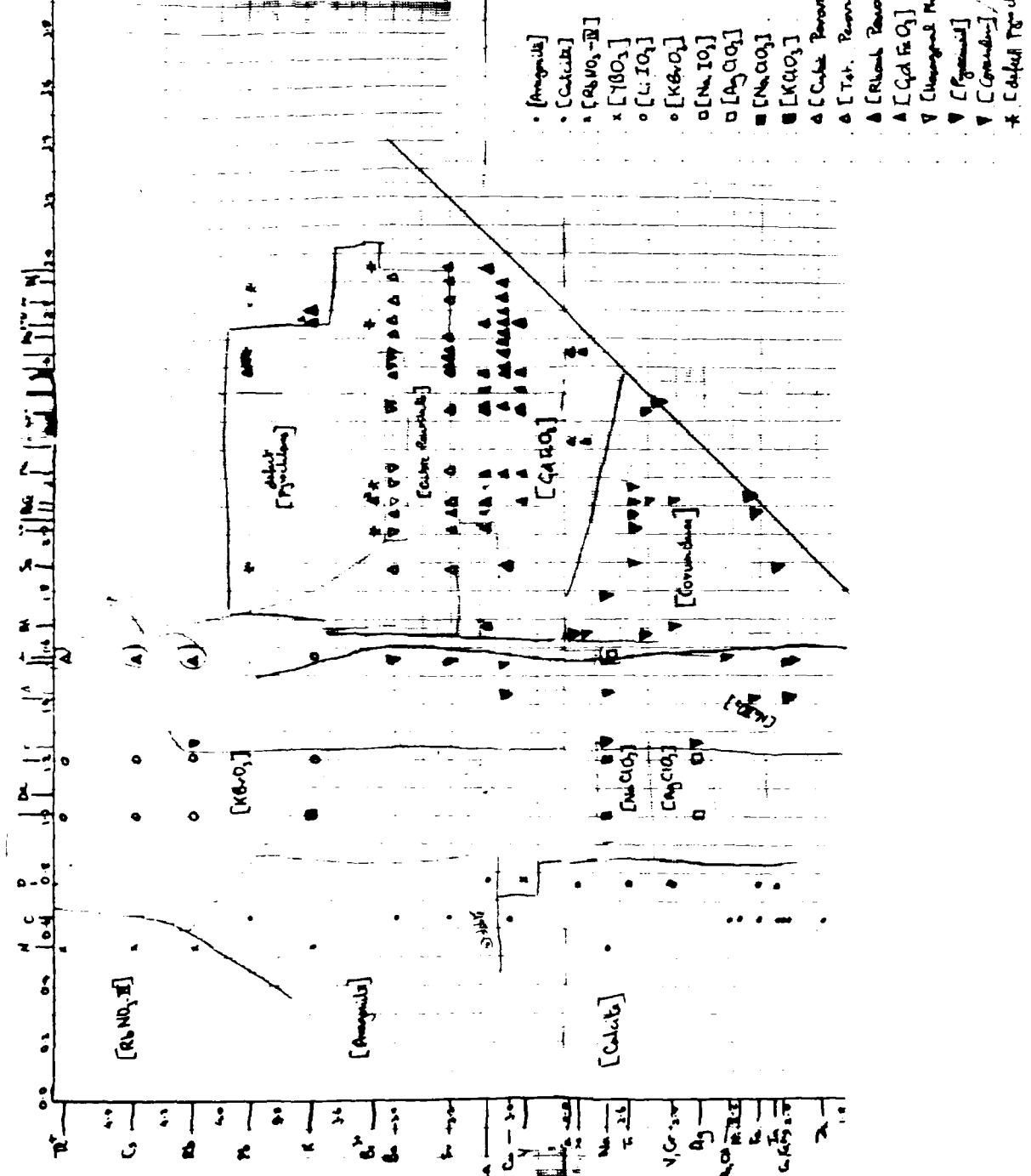
- $\beta-K_2SO_4$
- α - Olivine
- β - $[CaFe_2O_4]$
- γ - $[Mn_2S_3]$
- \square - $[Fe_3P]$
- ∇ - Thiomallite
- \blacksquare - Spinel
- $/$ - Ca_3S_4
- \blacktriangle - $[Co_2Fe_2S_4]$
- \blacktriangle - $PbCr_2S_4$
- \blacktriangledown - $PbCr_2S_4$

Sulfides, Selenides, Tellurides

$[\beta-K_2SO_4]$

This point separates CaY_2S_6 with the $Ca_2Y_2S_6$ structure, and $CaY(Co_2Te)_2$ with the $[CaMnS_2]$ structure.







A hand-drawn signature or code consisting of the letters 'D', 'T', 'T', and 'C' connected by a single horizontal line. The 'D' is on the left, followed by two 'T's, and finally a 'C' on the right.

A hand-drawn number consisting of the digit '7' followed by a short horizontal line and the digits '86'. The '7' is on the left, the line is in the middle, and '86' is on the right.